Recommendations for the Detection and Analysis of the ISO 12233:2023 e-SFR Slanted Star

Sarah Kerr; Imatest LLC; Boulder, Colorado USA

Abstract

The introduction of the new edge-based spatial frequency response (e-SFR) feature, known as the slanted star, in ISO 12233:2023 marks a significant change to the standard. This feature offers four additional edge orientations compared to the previously used slanted square, enabling measurement of sagittal and tangential spatial frequency response (SFR) in addition to SFR derived from vertical and horizontal edges. However, the expanded utility provided by these additional edges presents challenges in reliably automating the placement of appropriate regions of interest (ROIs) for e-SFR analysis, thereby complicating the accurate comparison of resolution across various orientations. This paper addresses these challenges by providing recommendations for the efficient and precise detection and analysis of the ISO 12233 slanted star feature. Our recommendations are based on thorough simulations and experimentally validated results obtained under diverse and challenging conditions.

Introduction

Measuring the spatial frequency response (SFR) of an imaging system is a critical aspect of evaluating the system's performance. The overall system response comprises the SFR of each of the system's individual components [1].Thus, understanding the distinct component contributions to the aggregate SFR is an essential aspect of image quality assessment and improvement.

System SFR anisotropy, the directional dependency of system response, offers a means to isolate component SFR contributions. For instance, in digital sensors which are typically composed of pixel rows and columns, vertical and horizontal SFR measurements naturally delineate system characteristics [1]. Likewise, optical component SFR is notably impacted by the inherent radial symmetry of lenses and their aberrations. Thus, evaluating sagittal (parallel to radius of curvature) and tangential (perpendicular to the radius) SFR measurements is preferable [2, 3].

ISO 12233:2023

The International Organization for Standardization (ISO) standard for resolution and spatial frequency response of electronic still picture imaging, known as ISO 12233 [3], defines terminology, test chart specifications, and test methods for performing resolution measurements. The standard features three distinct methodologies: visual resolution measurement using a hyperbolic wedge test pattern, edge-based spatial frequency response (e-SFR) measurement using low contrast slanted edges, and sine-based spatial frequency response (s-SFR) measurement using the sine wave-modulated starburst pattern.

While the visual resolution and s-SFR measurements have remained unchanged from previous versions of the standard [4], the e-SFR measurement has been updated significantly for the 2023 ISO 12233 edition 4 publication. Several changes to the e-SFR algorithm have been made to increase SFR accuracy [5].

Figure 1. *(left) ISO 12233:2017 slanted square. (right) ISO 12233:2023 four-cycle slanted star.*

e-SFR overview and updates

The comprehensive e-SFR measurement is extensively described in the ISO 12233 standard and additional literature [3, 5, 6, 7, 8]. However, the abridged algorithm can be described in several key steps: (1) measurement of the edge spread function (ESF), (2) differentiation of the ESF to obtain the line spread function (LSF), and (3) Fourier transform of the LSF to derive the frequency dependent SFR. Brief descriptions of updates to the e-SFR algorithm for ISO 12233:2023 are described below.

Accurate measurement of the ESF is limited by the precision of the 4x oversampled binning orthogonal to the direction of the detected edge. The misalignment between the pixel geometry and edge orientation leads to a discrepancy between pixel pitch and bin size. A cosine correction to compensate for the difference between these two widths leads to a more precise ESF and can be propagated through steps (1) and (2) to be applied directly to the SFR domain as shown in annex D of ISO 12233:2023 [9].

Furthermore, the ESF is also more accurately characterized in the 4th edition of ISO 12233 via a 5th order polynomial fit to the edge, rather than the previously used linear fit. This is largely beneficial for slanted edge analysis of curved edges in imaging systems with significant geometric distortion [10].

The last significant update to the e-SFR algorithm for ISO 12233:2023 is the choice of a Hann window over the previously used Hamming window. The Hann window is applied to the ESF in step (1) to remove contributions from low frequency non-uniformities, and also applied to the LSF for apodization prior to step (3), with a more aggressive high frequency roll off compared to the Hamming window.

For a thorough analysis and discussion of the updated e-SFR algorithm, see Burns et al. [5].
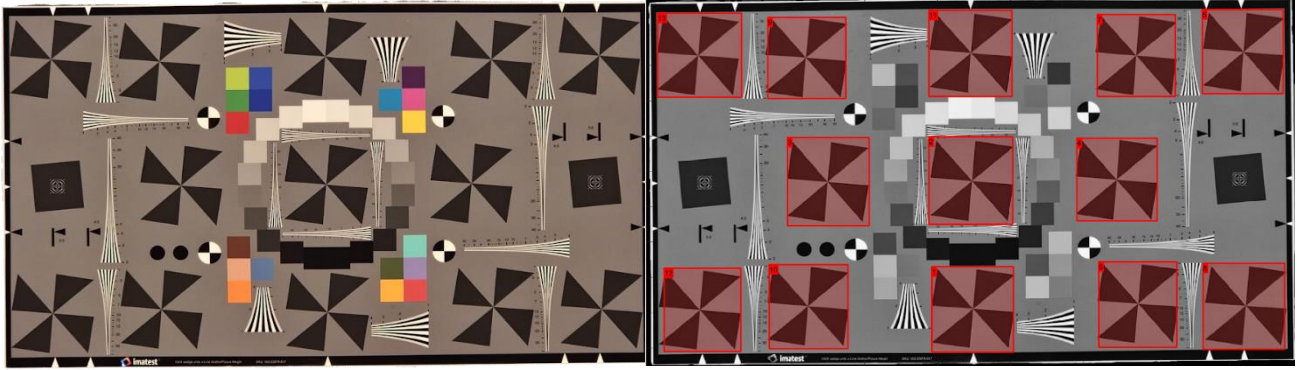
Figure 2. *(Left) ISO 12233:2023 e-SFR compliant test chart. The middle nine stars are required by the standard. Four additional stars in the corners provide additional e-SFR measurements. Chart image enhanced from standard version, copyright Imatest and reproduced with permission. (Right) Localized slanted stars on an ISO 12233:2023 compliant test chart.*

From slanted square to slanted star

The introduction of the slanted star (see Fig. 1) in ISO 12233:2023 as an edge-based spatial frequency response test pattern marks a significant update to the standard. Its diagonal edges complement established horizontal and vertical edges, enabling more comprehensive sampling of sagittal and tangential SFR performance across the imaging system's field of view. However, leveraging the slanted star presents unique challenges in automatically placing suitable regions of interest (ROIs) along each slanted edge, a prerequisite of implementing the e-SFR algorithm. These challenges stem from increased difficulty in detecting slanted stars under diverse imaging conditions and the precise fitting of ISO 12233:2023 compliant rectilinear ROIs amidst the acute angles of the star test pattern. Consequently, achieving a thorough and effective assessment of system SFR via the four-cycle slanted star necessitates advanced detection techniques that surpass the reliability and accuracy previously required by the slanted square.

Slanted Star Detection

Step (1) of the e-SFR algorithm as defined in the ISO 12233:2023 standard is for a user to select a rectangular region of interest for each slanted edge. Given that ISO 12233:2023 requires a minimum of nine slanted stars for a thorough e-SFR analysis (see Fig. 2), a minimum of 72 ROIs must be considered per image. This quickly becomes challenging as testing parameters scale, increasing the number of images to be considered for analysis. Thus, robust, reliable, and quick automatic detection of the slanted stars and placement of ISO 12233:2023 compliant ROIs becomes a requirement for practical analysis. This can be accomplished in four main steps: slanted star localization, slanted star center detection, slanted star edge detection, and slanted edge ROI placement.

Slanted Star Localization

A convolutional neural net was trained to localize individual slanted stars from a complex scene using OpenCV [7] and PyTorch [8] in Python. Universal Data Tool [9] was used to label the training data, which was augmented with noise, blur, distortion, translations, rotations, and reflections via Albumentations [10]. The goal of the model was to localize each slanted star in a scene within a rectangular bounding box (see Fig. 2). More specific training for slanted star center localization and edge detection was prohibitively tedious and unnecessary since

bounding boxes were found to be sufficient to proceed with traditional image processing techniques.

Slanted Star Center

The geometric form and two-tone coloring of the four-cycle slanted star makes the novel application of two one-dimensional Walsh-Hadamard transforms ideal for detection. The Walsh-Hadamard transform is a generalized Fourier transform which converges more quickly and with less error for binary signal reconstruction [11]. The sequential Walsh-Hadamard basis describes a greater number of binary transitions as the order increases. The zeroth order term is a DC offset, the first order term corresponds to a single transition, the second order term corresponds to two transitions, and so on (See Fig. 3). It becomes apparent that the four-cycle slanted star can be described accurately via the zeroth and the fourth order terms. In particular, when performing a Walsh-Hadamard transform along x or y, we expect the first boundary of the star to be defined by a decrease in the DC energy and an increase
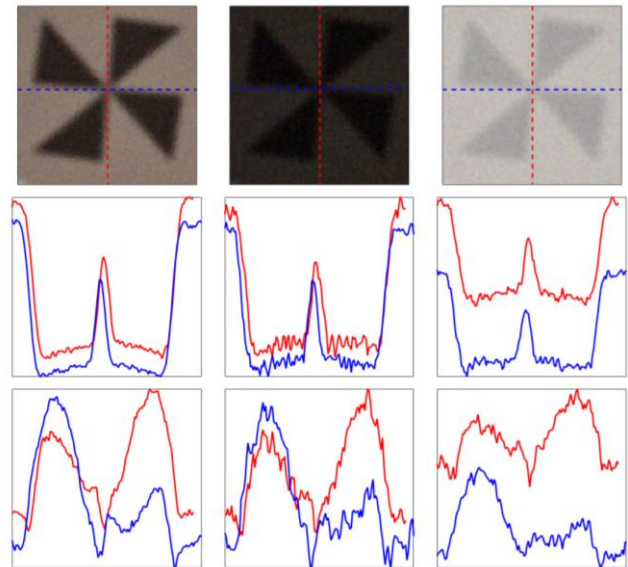

Figure 3. *(top) Example center detection of stars in blurry, low contrast, noisy scenarios with x localization in red and y localization in blue. (middle) Walsh-Hadamard transform zeroth order local maxima to indicate center with x in red and y in blue. (bottom) Fourth order local minima to indicate center with x in red and y in blue.*

	SNR (dB)					
	1.5	2.4	3.9	6.2	10	Inf
Extreme Pincushion	73%	70%	77%	80%	83%	100%
Pincushion	90%	100%	100%	100%	100%	100%
Undistorted	97%	98%	97%	100%	100%	100%
Barrel	93%	93%	90%	100%	100%	100%
Extreme Barrel	83%	83%	87%	90%	100%	100%

Figure 4. Coverage probability for center detection of four-cycle slanted stars for given distortion and noise SNR. Percents indicate what fraction of stars for each condition fell within 1% (normalized by average half width/height) of the expected location.

in the fourth order energy, then the center of the star is characterized by a local maxima in the DC term and a local minima in the fourth order term, and finally the second boundary of the star will appear as an increase in the DC energy and a decrease in the fourth order energy. Thus, the center of each star can be reliably found by looking for local extrema in the zeroth and fourth order Walsh-Hadamard terms (see Fig. 3).

To test the detection accuracy, an ensemble of artificially degraded slanted star images was generated by adding arbitrary rotations, radial distortion, Gaussian blur, and white Gaussian noise to an ideal 4:1 contrast four-cycle slanted star. The radial distortion was applied to stars at a normalized radial distance of 0.7, using a tangent model to simulate barrel distortion ($p = 0.075, 0.15$) and an arctangent model to simulate pincushion distortion ($p = -0.06, -0.12$) [12]. The added Gaussian blur had standard deviation ranging from 0.5 to 3, all with a kernel size of 15. The noise was added to yield images with signal to noise ratios of 1.5, 2.4, 3.9, 6.2, and 10 dB. Success was measured by considering the coverage probability of correctly detecting the slanted star center within 1% relative error, normalized by average star half width/height for each radial distortion condition. Results are shown in Figure 4 and sample stars are shown in Annex A.

Slanted Star Edges

Prior knowledge of the location of the slanted star centers makes it possible to reliably and consistently detect the slanted star edges via a polar binning of the slanted star signal. Polar bins are created centered about the slanted star center, at a spacing of 2 degrees, with a constant radius typically smaller than the slanted star (see Fig. 5). All of the pixels in each bin are summed and then edge detection is performed on the signal as a function of polar angle, with the assumption that the edges are relatively equally spaced apart from each other.

To test edge detection success, edge detection was performed upon the same ensemble of sample images which were used for center detection. These images were artificially degraded with radial geometric distortion, blur, and noise. The number of true positives, false positives, and false negatives were counted for each star. The precision, recall, and F-Score were then calculated (see Fig. 6). There was perfect edge detection for all of the stars without any
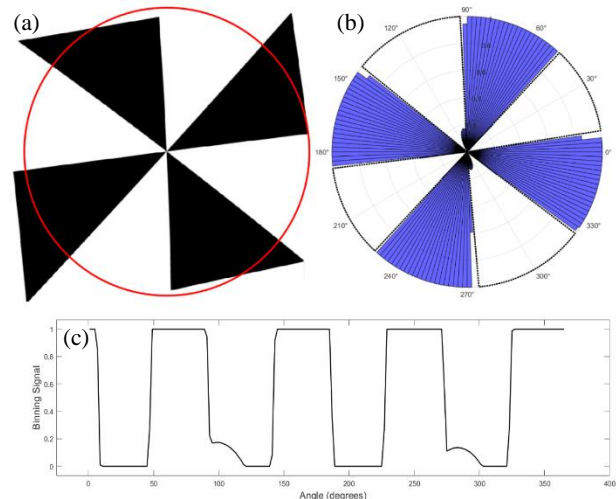

Figure 5. (a) Slanted star with pincushion distortion. Sampled area shown in red. (b) Polar binning of slanted star signal at 2 degree increments. (c) Polar binning signal upon which edge detection can be reliably performed.

distortion and all of the stars with slight pincushion distortion. Slanted stars with slight barrel distortion, extreme pincushion distortion, and extreme barrel distortion had lower rates of detection success. This can be explained by the assumption that the edges are relatively equally spaced apart from each other, which works well for undistorted or low distorted scenarios, but compromises edge detection when distortion is present.

Slanted Edge ROIs

Successful slanted star localization, center detection, and edge detection allows for the automatic placement of appropriate ROIs throughout the image. According to ISO 12233:2023, an e-SFR ROI must contain a slanted edge and should have vertical and horizontal sides between 100 and 400 pixels per side, with exceptions allowed with appropriate reporting. The slanted edge must intersect opposite sides of the ROI. That is, either the top and the bottom sides, or the right and the left sides. Although not a requirement of ISO 12233:2023, there is consensus that the edge should intersect the short sides of the ROI [18, 19] (see Fig. 7c). This recommendation is easily adopted for slanted edges from the slanted square and also for the vertical and horizontal edges of the four-cycle slanted star. However, placement of an ISO 12233:2023 compliant ROI on any of the diagonal edges of the four-cycle slanted star requires that the edge must intersect the long dimension of the rectangular ROI (see Fig. 7d), leading to inconsistent SFR results.

Future Work

Alternative ROI shapes should be considered to better suit the geometry of the four-cycle slanted star and its edges. Masaoka et al have shown that arbitrarily shaped ROIs produce accurate SFR measurements when the bins are properly normalized during ESF fit

	True Positives	False Positives	False Negatives	Precision	Recall	F-score
Extreme Pincushion	438	42	714	91.3%	38.0%	53.7%
Pincushion	1440	0	0	100.0%	100.0%	100.0%
Undistorted	2880	0	0	100.0%	100.0%	100.0%
Barrel	1369	71	71	95.1%	95.1%	95.1%
Extreme Barrel	864	204	584	80.9%	59.7%	68.7%

Figure 6. Edge detection for slanted stars for given distortion

[7]. Thus, non-rectangular ROIs which are better suited to the shape of the four-cycle slanted star should be considered for inclusion in future revisions of ISO 12233. Some promising variations include slanted rectangles and wedge-shaped ROIs (see Fig. 8).

Alternative slanted edge targets, which prioritize sagittal and tangential SFR measurements, could also be considered for inclusion in future revisions of ISO 12233:2023.

Conclusion

The introduction of the four-cycle slanted star feature in ISO 12233:2023 has enabled a more nuanced and comprehensive analysis of SFR across imaging systems. By incorporating four additional edge orientations, the slanted star pattern allows for comparison between sagittal, tangential, vertical, and horizontal SFR measurements across the field of view. Despite the challenges associated with automating the placement of ROIs for effective e-SFR analysis, this paper has outlined practical solutions to overcome these hurdles, thereby facilitating a more accurate and efficient evaluation of imaging system resolution across various orientations.

Through a combination of thorough simulations and experimental validations under diverse conditions, we have demonstrated that the detection of the slanted star feature and ROI placement can be conveniently automated. By employing advanced techniques such as convolutional neural networks for star localization, Walsh-Hadamard transforms for center detection, and polar binning for edge detection, we have established a robust methodology for automatically placing ISO 12233:2023 compliant ROIs with high precision and reliability.

However, this work also highlights the necessity for future revisions of the ISO standard to consider alternative ROI shapes and slanted edge targets that better accommodate the geometry of the slanted star. This will not only address the inconsistencies in SFR results but also enhance the standard's applicability to a wider range of imaging scenarios.

As imaging technology continues to evolve, it is imperative that standards like ISO 12233 adapt to these changes by embracing novel methodologies and test patterns. The slanted star feature is a testament to the standard's ongoing refinement and its commitment to providing a comprehensive framework for image quality assessment. By addressing the challenges associated with this advancement, we can unlock the full potential of ISO 12233:2023, paving the way for even more comprehensive and convenient targets in the future.
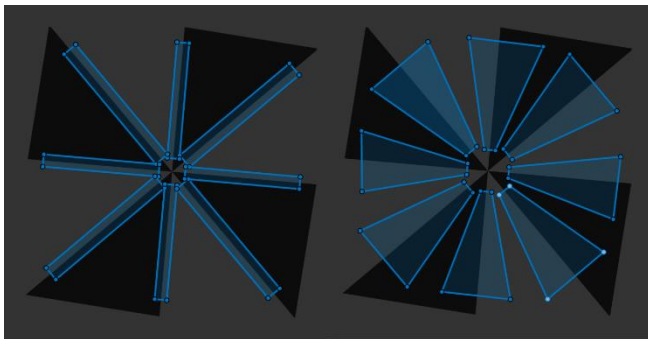
Figure 8. *Alternative ROIs that can be considered for future revisions of ISO 12233:2023.*
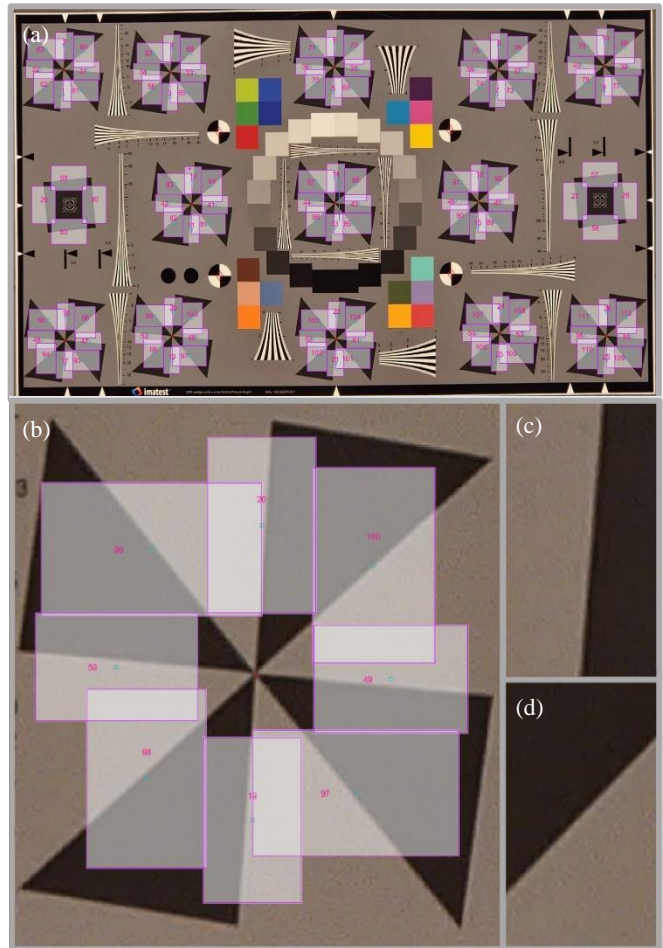
Figure 7. *(a) Successful slanted star localization, center detection, and edge detection allows for the automatic placement of ISO 12233:2023 compliant ROIs. Chart image enhanced from standard version, copyright Imatest and reproduced with permission. (b) The acute angles between neighboring edges on the interior of the four-cycle slanted star make it difficult to place consistent ROIs. (c) ISO 12233:2023 compliant ROI corresponding to the top vertical edge of the four-cycle slanted star. This ROI follows best practices. (d) ISO 12233:2023 compliant ROI corresponding to the top right diagonal edge of the four-cycle slanted star. This ROI does not follow best practices.*

References

[1] Keelan, Handbook of Image Quality, CRC Press, 2002, p. 209.

[2] Hecht and Zajac, Optics, Addison Wesley Publishing Company, 1974, pp. 180-182.

[3] Phillips and Eliasson, Camera Image Quality Benchmarking, John Wiley & Sons, 2018.

[4] *ISO 12233:2023, Photography—Electronic still picture imaging — Resolution and spatial frequency responses,* ISO, 2023.

[5] Parulski, Wueller, Burns and Yoshida, "Creation and Evolution of ISO 12233, the International Standard for Measuring Digital Camera Resolution," in *IS&T International Symposium on Electronic Imaging 2022, Image Quality and System Performance XIX*, 2022.

[6] Burns, Masaoka, Parulski and Wueller, "Updated Camera Spatial Frequency Response for ISO 12233," in *IS&T International Symposium on Electronic Imaging 2022, Image Quality and System Performance XIX*, 2022.

[7] Koren, "Sharpness: What is it and How is it Measured," Imatest LLC, [Online]. Available: https://www.imatest.com/docs/sharpness/#slant_algorithm.

[8] Masaoka, "Accuracy and Precision of Edge-Based Modulation Transfer Function," *IEEE Access,* vol. 6, pp. 41079-41086, 2018.

[9] Masaoka, Yamashita, Nishida and Sugawara, "Modified slanted-edge method and multidirectional modulation transfer function estimation," *Optics Express,* vol. 22, no. 5, 2017.

[10] Roland, "A Study of Slanted-Edge MTF Stability and Repeatability," 2015. [Online]. Available: https://www.imatest.com/wp-content/uploads/2015/02/Slanted-Edge_MTF_Stability_Repeatability.pdf.

[11] Burns and Williams, "Camera Resolution and Distortion: Advanced Edge Fitting," in *IS&T International Symposium on Electronic Imaging 2018 Image Quality and System Performance XV*, 2018.

[12] "OpenCV," OpenCV Team, 2024. [Online]. Available: https://opencv.org/.

[13] "PyTorch," The Linux Foundation, [Online]. Available: https://pytorch.org/.

[14] "Universal Data Tool," Open Human Annotation, [Online]. Available: https://universaldatatool.com/.

[15] Buslaev, Iglovikov, Khvedchenya, Parinov, Druzhinin and Kalinin, "Albumentations: Fast and Flexible Image Augmentations," *Information,* vol. 11, 2020.

[16] Kunz, "On the Equivalence Between One-Dimensional Discrete Walsh-Hadamard and Multidimensional Discrete Fourier Transforms," *IEEE Transactions on Computers,* vol. 28, no. 3, pp. 267-268, 1979.

[17] Koren, "Distortion: methods and modules," Imatest LLC, [Online]. Available: https://www.imatest.com/docs/distortion-methods-and-modules/.

[18] Wu, Xu, Piao and Yue, "Analysis of Edge Accuracy and Practical Multidirectional Modulation Transfer Function Measurement," *Applied Sciences,* vol. 12, no. 12748, 2022.

[19] Koren, "Using SFR part 2: Running Imatest SFR," Imatest LLC, [Online]. Available: https://www.imatest.com/docs/sfr_instructions2/.

[20] Koren, "Imatest ISO 12233 Edge SFR Chart," [Online]. Available: https://www.imatest.com/product/iso12233/.

Author Biography

Sarah Kerr received her B.S. in physics from the University of Maryland - College Park (2018) and her M.S. in physics with an applied physics specialization in imaging sciences from the University of Colorado, Boulder (2021). Since then, she has worked at Imatest LLC in Boulder, Colorado as an imaging scientist where she is involved with several international standards and industry efforts such as ISO 12233, IEEE P2020, and VCX.

Annex A

Subset of slanted stars considered for localization, center detection, and edge detection with varying levels of geometric distortion and signal to noise ratio.